DOI: 10.19884/j.1672-5220.202403001

Enhancing Piezoelectric Output via Constrained Phase Separation on Single Nanofibers: Harnessing Endogenous Triboelectricity

YU Dingming[1,2], LIU Lifang[1,2], YU Jianyong[1,2], SI Yang[1,2*], DING Bin[1,2*]
1. College of Textiles, Donghua University, Shanghai 201620, China
2. Innovation Center for Textile Science and Technology, Donghua University, Shanghai 201620, China

Abstract: The research, fabrication and development of piezoelectric nanofibrous materials offer effective solutions to the challenges related to energy consumption and non-renewable resources. However, enhancing their electrical output still remains a significant challenge. Here, a strategy of inducing constrained phase separation on single nanofibers via shear force was proposed. Employing electrospinning technology, a polyacrylonitrile/polyvinylidene difluoride (PAN/PVDF) nanofibrous membrane was fabricated in one step, which enabled simultaneous piezoelectric and triboelectric conversion within a single-layer membrane. Each nanofiber contained independent components of PAN and PVDF and exhibited a rough surface. The abundant frictional contact points formed between these heterogeneous components contributed to an enhanced endogenous triboelectric output, showcasing an excellent synergistic effect of piezoelectric and triboelectric response in the nanofibrous membrane. Additionally, the component mass ratio influenced the microstructure, piezoelectric conformation and piezoelectric performance of the PAN/PVDF nanofibrous membranes. Through comprehensive performance comparison, the optimal mass ratio of PAN to PVDF was determined to be 9∶1. The piezoelectric devices made of the optimal PAN/PVDF nanofibrous membranes with rough nanofiber surfaces generated an output voltage of 20 V, which was about 1.8 times that of the smooth one at the same component mass ratio. The strategy of constrained phase separation on the surface of individual nanofibers provides a new approach to enhance the output performance of single-layer piezoelectric nanofibrous materials.

Keywords: nanofibrous membrane; constrained phase separation; endogenous triboelectric effect; dual-component; piezoelectric property
CLC number: TS171 **Document code**: A
Article ID: 1672-5220(2025)01-0012-08

Open Science Identity (OSID)

0 Introduction

The extensive consumption of fossil fuels and associated environmental concerns have garnered global attention, driving researchers to explore alternative renewable energy sources including bioenergy, hydrogen energy and mechanical energy[1-3]. Among these, mechanical energy stands out as a readily available source, and the emerging piezoelectric materials excel at harvesting mechanical energy and converting it into electricity[4]. Novel piezoelectric nanogenerators (PENGs) developed based on this demonstrate significant potential for various applications in wearable sensors[5], implantable health monitoring devices[6], energy storage[7], etc. However, it is important to highlight that their electrical output currently remains modest.

Extensive research has been conducted to enhance the electrical output of PENGs[8-9]. Traditional ceramic-based piezoelectric materials, such as zinc oxide and barium titanate, have been widely used for mechanical energy conversion. However, these materials still suffer from poor structural flexibility, which often leads to brittle fractures or fatigue cracks[10]. In contrast, polymeric piezoelectric materials, exemplified by polyvinylidene difluoride (PVDF), offer excellent flexibility and piezoelectric performance. However, with the continuous evolution of electronic devices, conventional PVDF-based PENGs with limited output performances face challenges in meeting the increasing energy consumption requirements[11]. It has been demonstrated that maximizing the proportion of the ferroelectric β-phase and achieving proper polarization direction are crucial strategies to address this issue[12]. Electrospinning enables the efficient fabrication of self-polarized PVDF nanofibers, characterized by a high β-phase content, attributed to the strong mechanical stretching forces generated by high electric fields[13]. However, further enhancing the electrical output of PENGs remains a daunting challenge.

Currently, most PENGs based on electrospun nanofibers consist of a single polymer component, and the piezoelectric conversion is mainly attributed to the

Received date: 2024-03-09
Foundation items: National Natural Science Foundation of China (No. 52373281); National Energy-Saving and Low-Carbon Materials Production and Application Demonstration Platform Program, China (No. TC220H06N)
* Correspondence should be addressed to DING Bin, email: binding@dhu.edu.cn; SI Yang, email: yangsi@dhu.edu.cn
Citation: YU D M, LIU L F, YU J Y, et al. Enhancing piezoelectric output via constrained phase separation on single nanofibers: harnessing endogenous triboelectricity [J]. *Journal of Donghua University (English Edition)*, 2025, 42(1): 12-19.

deformation of nanofibers[14]. In contrast, triboelectric nanogenerators (TENGs) operate by converting mechanical energy into electrical energy through the electrostatic induction and triboelectric coupling effect[15]. It should be noted that the electrical output of TENGs is typically higher than that of PENGs. In order to enhance the electrical output of nanofibrous membranes, considering the simultaneous occurrence of inter-fiber contact and slip phenomena during the compression, a promising approach involves constructing multi-component fibers within a single-layer membrane[16]. This enables the generation of additional frictional charges through the frictional contact between different fibers. Considering the cumulative output of triboelectric effects, polyacrylonitrile (PAN) with its excellent stability, piezoelectric performance and high positive charge affinity is selected as the optimal polymer phase[17]. However, the fiber-to-fiber contact in the membrane mainly consists of point contacts, limiting the effective contact points between the heterogeneous polymer single fibers. To address this issue, researchers have employed co-electrospinning of PAN and PVDF to prepare nanofibrous membranes incorporating both heterogeneous components within a single fiber to enhance inter-fiber friction points[18]. However, the smooth surface of these nanofibers constrains further increase in contact points.

In this work, we design dual polymer phases within single nanofibers featuring a rough groove surface through surface-constrained phase separation. During the electrospinning process, the jet containing both PVDF and PAN undergoes shear-induced phase separation on the surface of individual nanofibers under high-speed whipping, leading to numerous frictional contact points between dual components within single nanofibers and among nanofibers. This significantly enhances the endogenous triboelectric effect, resulting in the membrane exhibiting superior piezoelectric output performance compared to the dual-component single nanofiber with a smooth surface. Furthermore, we investigate the impact of the component mass ratio in nanofibers on the microstructure, piezoelectric conformation and piezoelectric performance of membranes, and validate the enhancement mechanism of the endogenous triboelectric effect in rough dual-component nanofibers.

1 Materials and Methods

1.1 Materials

PAN (M_r = 149 000 – 151 000), PVDF (M_r = 320 000), *N*, *N*-dimethylformamide (DMF) and acetone were all obtained from Shanghai Titan Technology Co., Ltd., China. Polyethylene terephthalate (PET) film and aluminum foil were bought from Taizhou Tongjida New Material Co., Ltd., China.

1.2 Fabrication of PAN/PVDF nanofibrous membranes

The preparation procedure of PAN/PVDF nanofibrous membranes is displayed in Fig. 1. Firstly, PAN powder was dissolved into DMF and stirred at room temperature for 8 h. Subsequently, PVDF powder was introduced into the solution, and the resulting mixture was stirred at 80 ℃ in a water bath for another 6 h, obtaining a uniform spinning solution. The total polymer mass fraction in the resulting solution was 14%, and the mass ratio of PAN to PVDF was 5∶5, 7∶3 and 9∶1, respectively. Additionally, pure PAN and pure PVDF solutions at equivalent mass fraction were prepared using the same method. Five syringes were used to individually extract 8 mL spinning solution for electrospinning. The applied voltage was 23 kV, accompanied by a feed rate of 1.2 mL/h and a receiving distance of 15 cm. The aluminum foil as the receiving substrate was wrapped around the drum rotating at 100 r/min. Throughout the process, the temperature was (25±2) ℃ and the relative humidity was (40 ± 5)%. Each solution underwent a spinning time of 3 h, then the obtained membranes were dried at 70 ℃ to remove residual DMF. Based on the mass ratio of PAN to PVDF in the spinning solution, the nanofibrous membranes were named N_xF_y, where N and F represent PAN and PVDF, respectively; *x* and *y* represent the mass proportions of PAN and PVDF, respectively.

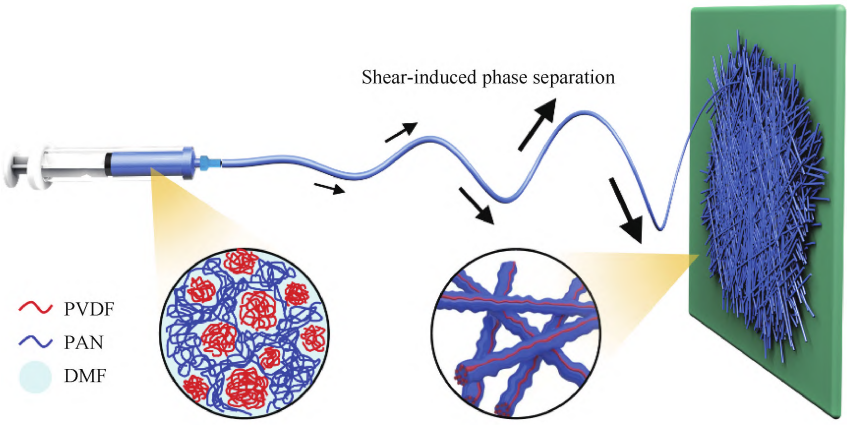

Fig. 1 Schematic diagram of PAN/PVDF nanofibrous membrane fabrication via electrospinning

The PAN/PVDF nanofibrous membranes with a smooth nanofiber surface were obtained by a similar process as mentioned above, with the differences that PAN and PVDF powders (the mass ratio of PAN to PVDF was 9∶1) were dissolved in a mixed solvent of DMF and acetone at a volume ratio of 4∶6, and the applied voltage during electrospinning was adjusted to 15 kV. The thickness and the nanofiber diameter of the nanofibrous membranes were controlled to be similar to those of rough PAN/PVDF nanofibrous membranes.

1.3 Piezoelectric property test

The nanofibrous membrane was assembled into a piezoelectric device as shown in Fig. 2, and its performance was tested. First, the nanofibrous membrane was cut into a square sample with a size of 4 cm×4 cm. Then, aluminum foil was used as electrodes and tightly attached to both sides of the nanofibrous membrane, with slightly smaller dimensions to prevent any formation of conductive paths. Finally, the entire device was coated and secured with PET film, ensuring that each layer was tightly adhered to the adjacent layer without any gaps. The assembled device was attached to an acrylic board that connected with a force gauge. A motor was used to cyclically impact the device in a vertical direction, with the motor speed adjusted to apply a pressure of approximately 10 N. The electrostatic meter (Keithley 6514, Tektronix, USA) was connected to the extended part of the aluminum foil to collect the voltage signals generated by the device, and the data was recorded using LabVIEW software.

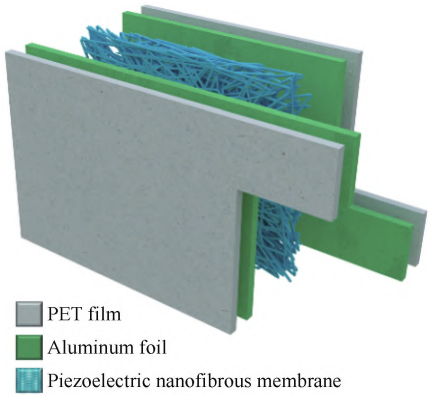

Fig. 2 Schematic diagram of piezoelectric device assembly

1.4 Characterization

A scanning electron microscope (SEM) (SU8010, Hitachi, Japan) was employed to observe the microscopic morphologies of nanofibers. A Fourier transform infrared (FTIR) spectroscope (Nicolet 6700, Thermo Fisher, USA) was applied to determine the content of piezoelectric conformation. X-ray diffraction (XRD) (D8 Advance, Bruker, Germany) was used to analyze the crystal structures of the nanofibrous membranes.

2 Results and Discussion

2.1 Morphology control and analysis of nanofibrous membranes

Different morphologies of nanofibrous membranes were achieved by adjusting the mass ratio of PAN to PVDF (Fig. 3). Notably, the nanofibers in N_5F_5 exhibit random orientation with some fine nanofibers, indicating a low uniformity in the nanofiber diameter. This can be attributed to the instability of the jet during the electrospinning process. As the PAN mass fraction in the solution progressively increases, the content of fine nanofibers in the membrane decreases. This is a result of the higher viscosity of the spinning solution caused by the increased PAN mass fraction, resulting in the increased nanofiber diameter with a more uniform distribution. Further analysis of the nanofiber diameter, as shown in Fig. 4, reveals an increase in the diameter with increasing PAN mass fraction in the nanofibers. The average nanofiber diameters of N_5F_5, N_7F_3 and N_9F_1 are 468.9, 508.9 and 547.1 nm, respectively. Overall, the PAN/PVDF nanofibers have similar diameters, around 500 nm, which facilitates the subsequent analysis and comparison of their piezoelectric properties. Moreover, all the nanofiber surfaces exhibit rough groove structures, which arises from the phase separation of the two-phase polymer components in the spinning solution under the high-speed shearing force of the jet[19]. The energy-dispersive spectroscopy (EDS) mapping reveals that both elements N and F, representing PAN and PVDF respectively, are distributed on the surface of the nanofibers, demonstrating the coexistence of these two polymers within individual nanofibers (Fig. 5).

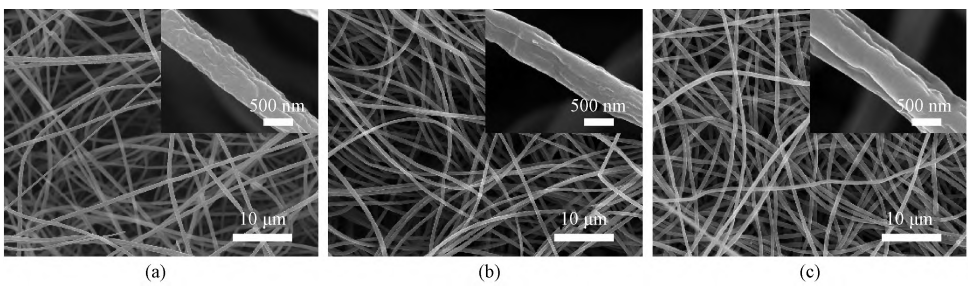

Fig. 3 SEM images of samples: (a) N_5F_5; (b) N_7F_3; (c) N_9F_1

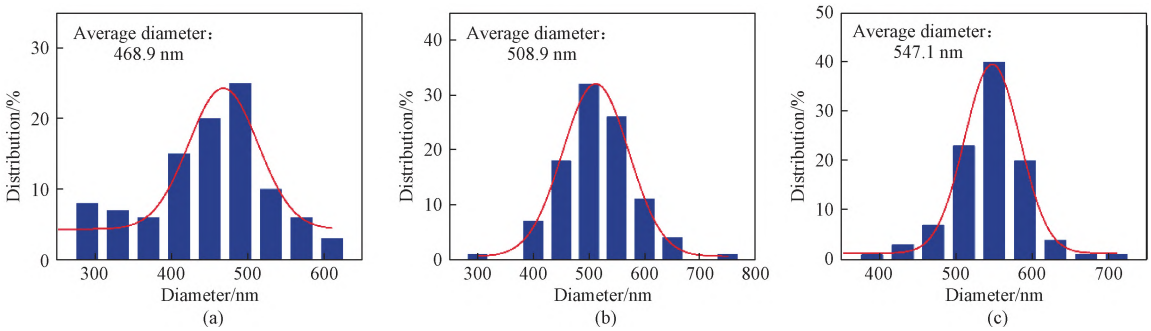

Fig. 4 Nanofiber diameter distributions of samples: (a) N_5F_5; (b) N_7F_3; (c) N_9F_1

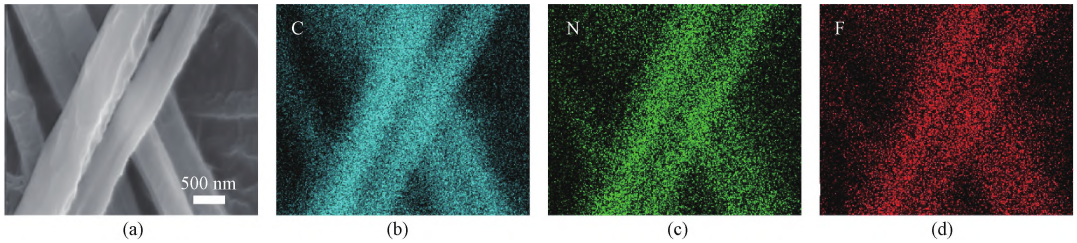

Fig. 5 EDS mappings of N_9F_1: (a) selected area; (b) C; (c) N; (d) F

2.2 Piezoelectric conformation analysis

The crystal structures of PAN/PVDF nanofibrous membranes, as well as PVDF nanofibrous membranes and PAN nanofibrous membranes, were characterized by XRD (Fig. 6). PVDF molecular chains exhibit the all-trans planar zigzag conformation, a defining feature of the β-phase known for its indispensable role in enhancing the excellent piezoelectric properties. The PVDF nanofibrous membranes show distinct β-phase diffraction peaks at $2\theta = 20.6°$, corresponding to the (110) and (200) crystal planes, indicating that the synergistic effect of mechanical stretching and in-situ polarization during the electrospinning process promotes the transformation to the β-phase[16]. PAN is an ethylene-based amorphous polymer with an all-trans planar zigzag conformation formed by the repulsive forces between neighboring cyano groups, enabling it to exhibit piezoelectric responsiveness. Characteristic peak corresponding to the (010) crystal plane of PAN is observed at $2\theta = 17.0$[20]. The PAN/PVDF nanofibrous membranes exhibit characteristic peaks at both 17.0° and 20.6° in the XRD patterns (Fig. 6(b)).

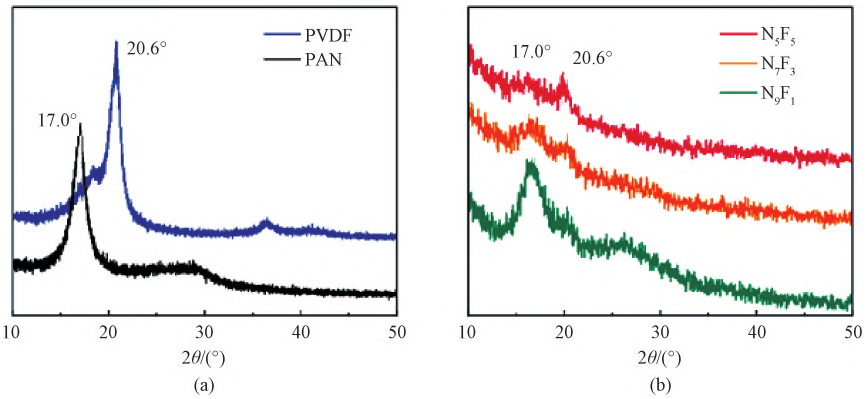

Fig. 6 XRD patterns of samples: (a) PVDF and PAN nanofibrous membranes; (b) PAN/PVDF nanofibrous membranes

Subsequently, further characterization analysis of the aforementioned nanofibrous membranes was performed using FTIR. In the FTIR spectra (Fig. 7), the peak at 840 cm^{-1} corresponds to the β-phase, while the peak at 763 cm^{-1} is indicative of the non-polar α-phase of PVDF.

The β-phase content of the membrane can be calculated as[21]

$$P_\beta = \frac{I_{840}}{(K_{840}/K_{763}) \times I_{763} + I_{840}} \times 100\%, \quad (1)$$

where P_β represents the content of β-phase; I_{840} and I_{763} denote the absorption intensities at the corresponding wavenumbers; K_{840} and K_{763} are the corresponding absorption coefficients, which are 7.7×10^4 cm^2/mol and 6.1×10^4 cm^2/mol, respectively.

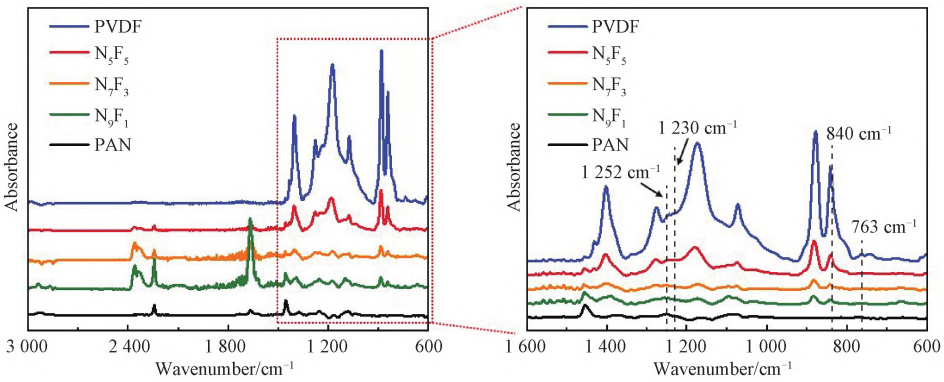

Fig. 7 FTIR spectra of PAN/PVDF, PVDF and PAN nanofibrous membranes

The calculated β-phase contents for PVDF nanofibrous membrane, N_5F_5, N_7F_3 and N_9F_1 are 90.62%, 88.58%, 68.75% and 71.01%, respectively. For PAN molecules, the vibrational bands at 1 252 cm^{-1} and 1 230 cm^{-1} in the FTIR spectrum correspond to its all-trans planar zigzag conformation and irregular helical conformation, respectively. Based on the FTIR spectrum, the content of the piezoelectric conformation is calculated as[21]

$$P_z = \frac{S_{1252}}{S_{1252} + S_{1230}} \times 100\%, \quad (2)$$

where P_z is the content of PAN all-trans planar zigzag conformation, representing the content of the piezoelectric conformation; S_{1252} and S_{1230} are the peak areas at 1 252 cm^{-1} and 1 230 cm^{-1}, respectively.

Due to the overlapping of PAN vibration bands at 1 252 cm^{-1} and 1 230 cm^{-1} with characteristic bands of PVDF, the peak-differentiating and imitating approach was employed to distinguish these peaks. The calculated contents of the piezoelectric conformation for PAN nanofibrous membrane, N_5F_5, N_7F_3 and N_9F_1 are 61.23%, 74.45%, 74.88% and 74.46%, respectively. The piezoelectric properties of piezoelectric polymers stem from the polarization of dipoles in the structure, and the calculation of the total dipole moment D in PAN/PVDF nanofibrous membranes is as follows[21]:

$$D = aD_1P_\beta + bD_2P_z, \quad (3)$$

where a and b represent the mass fractions of PVDF and PAN in the nanofibers, respectively; D_1 and D_2 are the dipole moments in the corresponding piezoelectric conformations of the polymers, $D_1 = 2.1$ Debye (D), and $D_2 = 3.5$ D.

The total dipole moments calculated for the PVDF nanofibrous membrane, N_5F_5, N_7F_3, N_9F_1 and PAN nanofibrous membrane are 1.90, 2.23, 2.27, 2.50 and 2.14 D, respectively. It can be concluded that N_9F_1 has the highest total dipole moment.

2.3 Piezoelectric property investigation

The trend of the output voltage of nanofibrous membranes is consistent with the trend in the total dipole moment, whereby a higher total dipole moment within the membrane results in a higher output voltage (Fig. 8). However, PAN/PVDF nanofibrous membranes only exhibit a 1.0–1.3 times increase in total dipole moments compared to the single-component nanofibrous membranes, yet the output voltage increases by 2.2–4.8 times. This can be attributed to the additive contribution of interfacial frictional polarization between PAN and PVDF components, induced by the phase separation on the individual nanofiber surface. Furthermore, the increase in the output voltage exhibited by PAN/PVDF nanofibrous membranes, with regard to varying polymer mass ratios, deviates from a linear correlation with the total dipole moment. This observation suggests a synergistic effect between the piezoelectric output from nanofiber deformation and the polarization via inter-polymer friction. Among the tested ratios, N_9F_1 demonstrates the highest output voltage (20 V), leading to the selection of N_9F_1 for further experimental analysis.

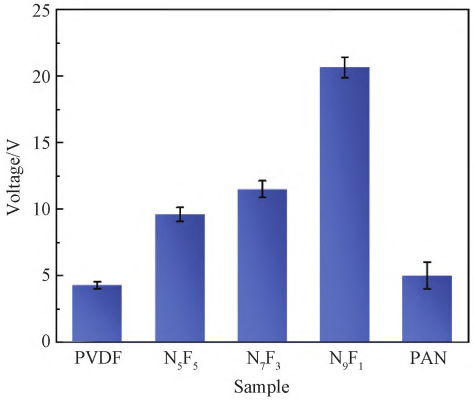

Fig. 8 Output voltages of PAN/PVDF, PVDF and PAN nanofibrous membranes

To further investigate the role of the rough surface on the individual nanofiber with dual components in increasing effective frictional contact points, we prepared a PAN/PVDF nanofibrous membrane with the same polymer mass ratio but different surface smoothness by adjusting the electrospinning voltage and solvent and compared the piezoelectric performance of the piezoelectric

devices made of them (Figs. 9 and 10). The results indicates that the rough PAN/PVDF nanofibrous membrane based piezoelectric device reaches an output voltage of 20 V, while the smooth one exhibits a lower output voltage of 11 V. The former is about 1.8 times of the latter. During friction, PAN is more susceptible to losing electrons compared to PVDF. The occurrence of lateral sliding and contact separation between these two polymers leads to negatively charged PVDF domains and positively charged PAN domains, with charge intensity dependent on the total number of contact points between the two components in the membrane[16]. It can be inferred that for nanofibrous membranes with the same thickness and nanofiber diameter, the rough surface of PAN/PVDF nanofibrous membrane provides more heterogeneous contact points, resulting in a larger total number of frictional contact points compared to the smooth one. Consequently, the piezoelectric device made of the PAN/PVDF nanofibrous membrane with rough nanofiber surface exhibits a superior output voltage.

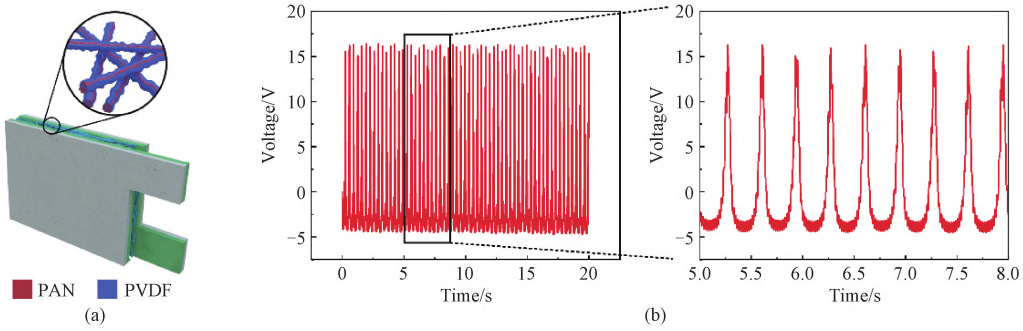

Fig. 9 Rough PAN/PVDF nanofibrous membrane based piezoelectric device and its piezoelectric performance: (a) schematic illustration of the piezoelectric device; (b) output voltage

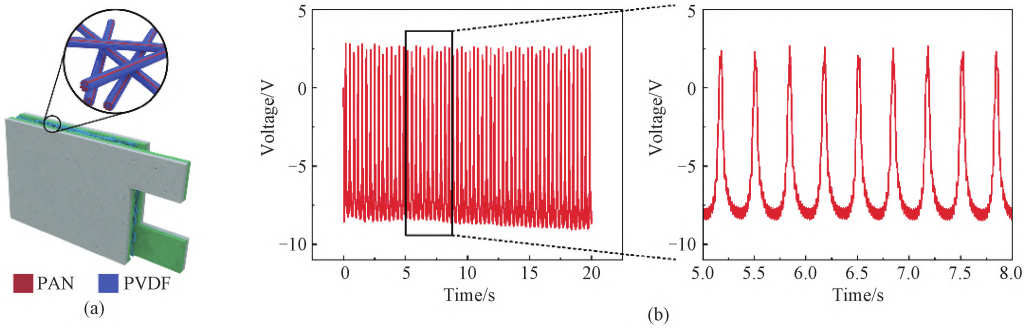

Fig. 10 Smooth PAN/PVDF nanofibrous membrane based piezoelectric device and its piezoelectric performance: (a) schematic illustration of the piezoelectric device; (b) output voltage

2.4 Mechanical performance investigation

The tensile performances of nanofibrous membranes are crucial for their potential applications in practical scenarios, such as the requirement to maintain structural integrity without damage when used as wearable sensors under stretching and deformation from body movements. As presented in the tensile stress-strain curves in Fig. 11, N_9F_1 achieves a superior tensile strength of 8.8 MPa, significantly surpassing both PVDF nanofibrous membranes (3.7 MPa) and PAN nanofibrous membranes (6.0 MPa). Additionally, N_9F_1 also exhibits the highest Young's modulus but displays a lower elongation (114.8%) at break compared to the PVDF and the PAN nanofibrous membranes. Therefore, PAN/PVDF nanofibrous membranes present superb mechanical properties for potential applications.

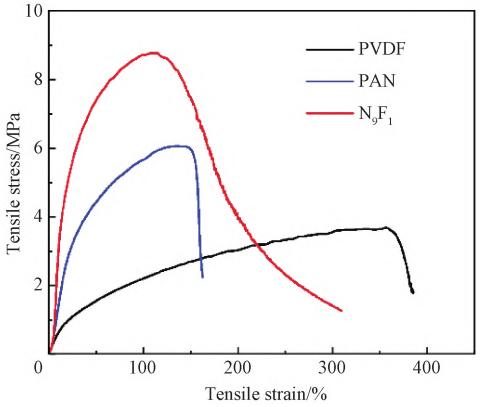

Fig. 11 Tensile stress-strain curves of N_9F_1, PVDF and PAN nanofibrous membranes

3 Conclusions

This study involved the preparation of nanofibrous membranes using shear-induced phase separation during electrospinning, resulting in individual nanofibers containing both PAN and PVDF components with a rough surface. Characterization and analysis were done on the membranes to evaluate their morphology, piezoelectric conformation and piezoelectric performance. The influence of the component mass ratio on morphology and piezoelectric performance was examined to determine the optimal parameters for the fabrication of PAN/PVDF nanofibrous membranes. The experimental results revealed that the phase separation of PAN and PVDF on the nanofiber surface resulted in the exposure of both polymer components. When subjected to external forces, the lateral sliding and contact separation between the rough nanofibers generated substantial endogenous triboelectric output. These effects, combined with the piezoelectric conversion, significantly enhanced the output voltage compared to the single-component nanofibrous membranes and the smooth PAN/PVDF nanofibrous membranes. Notably, at a PAN to PVDF mass ratio of 9 ∶ 1, the nanofibrous membrane based piezoelectric device exhibited the highest output voltage of 20 V.

References

[1] HUANG A, GUO Y, ZHU Y W, et al. Durable washable wearable antibacterial thermoplastic polyurethane/carbon nanotube@silver nanoparticles electrospun membrane strain sensors by multi-conductive network[J]. *Advanced Composites and Hybrid Materials*, 2023, 6(3): 101.

[2] RUI P S, ZHANG W, WANG P H. Super-durable and highly efficient electrostatic induced nanogenerator circulation network initially charged by a triboelectric nanogenerator for harvesting environmental energy[J]. *ACS Nano*, 2021, 15(4): 6949-6960.

[3] ZHANG F, YU J Y, SI Y, et al. Meta-aerogel ion motor for nanofluid osmotic energy harvesting [J]. *Advanced Materials*, 2023, 35(38): 2302511.

[4] LI J, LONG Y, YANG F, et al. Degradable piezoelectric biomaterials for wearable and implantable bioelectronics[J]. *Current Opinion in Solid State and Materials Science*, 2020, 24(1): 100806.

[5] PERSANO L, DAGDEVIREN C, SU Y W, et al. High performance piezoelectric devices based on aligned arrays of nanofibers of poly(vinylidenefluoride-co-trifluoroethylene)[J]. *Nature Communications*, 2013, 4: 1633.

[6] DAGDEVIREN C, SHI Y, JOE P, et al. Conformal piezoelectric systems for clinical and experimental characterization of soft tissue biomechanics[J]. *Nature Materials*, 2015, 14(7): 728-736.

[7] XU W, HUANG L B, HAO J H. Fully self-healing and shape-tailorable triboelectric nanogenerators based on healable polymer and magnetic-assisted electrode[J]. *Nano Energy*, 2017, 40: 399-407.

[8] FU J, HOU Y D, ZHENG M P, et al. Flexible piezoelectric energy harvester with extremely high power generation capability by sandwich structure design strategy[J]. *ACS Applied Materials & Interfaces*, 2020, 12(8): 9766-9774.

[9] CAO X L, XIONG Y, SUN J, et al. Piezoelectric nanogenerators derived self-powered sensors for multifunctional applications and artificial intelligence[J]. *Advanced Functional Materials*, 2021, 31(33): 2102983.

[10] HABIB M, LANTGIOS I, HORNBOSTEL K. A review of ceramic, polymer and composite piezoelectric materials[J]. *Journal of Physics D: Applied Physics*, 2022, 55(42): 423002.

[11] JIANG H W, SONG L, HUANG Z X, et al. A novel concept of hierarchical porous structural design on enhancing output performance of piezoelectric nanogenerator[J]. *Nano Energy*, 2022, 104: 107921.

[12] LI T, QU M H, CARLOS C, et al. High-performance poly(vinylidene difluoride)/dopamine core/shell piezoelectric nanofiber and its application for biomedical sensors [J]. *Advanced Materials*, 2021, 33(3): 2006093.

[13] LI T, FENG Z Q, QU M H, et al. Core/shell piezoelectric nanofibers with spatial self-orientated β-phase nanocrystals for real-time micropressure monitoring of cardiovascular walls [J]. *ACS Nano*, 2019, 13(9): 10062-10073.

[14] CURRY E J, LE T T, DAS R, et al. Biodegradable nanofiber-based piezoelectric transducer [J]. *Proceedings of the National Academy of Sciences of the United States of America*, 2020, 117(1): 214-220.

[15] WANG C Y, GUO H Y, WANG P, et al. An advanced strategy to enhance TENG output: reducing triboelectric charge decay[J]. *Advanced Materials*, 2023, 35(17): 2209895.

[16] HUANG A, ZHU Y W, PENG S Q, et al. Improved energy harvesting ability of single-layer binary fiber nanocomposite membrane for multifunctional wearable hybrid piezoelectric and triboelectric nanogenerator and self-powered sensors[J]. *ACS Nano*, 2024, 18(1): 691-702.

[17] WANG W Y, ZHENG Y D, JIN X, et al. Unexpectedly high piezoelectricity of electrospun polyacrylonitrile nanofiber membranes[J]. *Nano Energy*, 2019, 56: 588-594.

[18] ZHANG P P, TONG W S, LIANG C, et al. Enhancing the endogenous triboelectricity of a polylactic acid nanofiber film by controlling the MXene content and distribution[J]. *Journal of Materials Chemistry A*, 2022, 10(45): 24310-24319.
[19] ZHANG F, JIAO W L, SI Y, et al. Tailoring nanoporous-engineered sponge fiber molecular sieves with ternary-nested architecture for precise molecular separation[J]. *ACS Nano*, 2021, 15(8): 13623-13632.
[20] FURUSHIMA Y, NAKADA M, TAKAHASHI H, et al. Study of melting and crystallization behavior of polyacrylonitrile using ultrafast differential scanning calorimetry[J]. *Polymer*, 2014, 55(13): 3075-3081.
[21] SHAO H, WANG H X, CAO Y Y, et al. Single-layer piezoelectric nanofiber membrane with substantially enhanced noise-to-electricity conversion from endogenous triboelectricity[J]. *Nano Energy*, 2021, 89: 106427.

单纤维表面限域相分离增强内源性摩擦以提高压电输出

俞丁铭[1,2]，刘丽芳[1,2]，俞建勇[1,2]，斯　阳[1,2*]，丁　彬[1,2*]
1. 东华大学 纺织学院，上海 201620
2. 东华大学 纺织科技创新中心，上海 201620

摘　要：压电纳米纤维材料的研究、制造和发展可有效破解能源消耗和不可再生的难题，然而提高压电纳米纤维材料电力输出仍然存在重大挑战。为此，提出了剪切力诱导单纤维表面限域相分离的策略，利用静电纺丝技术一步制备出聚丙烯腈/聚偏氟乙烯（PAN/PVDF）纳米纤维膜，实现在单层纤维膜内同时进行压电和摩擦电转换。其单纤维内同时含有相对独立的 PAN 和 PVDF 两种组分且表面粗糙，形成的大量异相组分间摩擦接触点大幅提升了材料的内源性摩擦电输出，使纤维膜表现出优异的压电和摩擦电协同效应。此外，纳米纤维中两种组分的比例对纤维的微观形貌、聚合物压电构象和纤维膜的压电性能均产生一定的影响。通过综合性能对比得到 PAN 和 PVDF 的最佳质量比为 9∶1。由 PAN 与 PVDF 质量比为 9∶1且纤维表面粗糙的 PAN/PVDF 纳米纤维膜制成的压电装置可以产生高达 20 V 的峰值输出电压，约为聚合物组分比例相同但纤维表面光滑的 PAN/PVDF 纳米纤维膜制成的压电装置的 1.8 倍。所采用的单纤维表面限域相分离策略为提高单层压电纳米纤维材料的输出性能提供了新的思路。

关键词：纳米纤维膜；限域相分离；内源性摩擦效应；双组分；压电性能